Transport in Porous Media **28:** 253–284, 1997.

Onset of Mobilization and the Fraction of Trapped Foam in Porous Media

DAVID COHEN[1,⋆], T. W. PATZEK[2] and C. J. RADKE[1,⋆⋆]
[1] *Department of Chemical Engineering, Earth Sciences Division of the Lawrence Berkeley National Laboratory, University of California, Berkeley, U.S.A.*
[2] *Department of Materials Science and Mineral Engineering, Earth Sciences Division of the Lawrence Berkeley National Laboratory, University of California, Berkeley, U.S.A.*

(Received: 30 May 1996; in final form: 29 April 1997)

Abstract. Usually, foam in a porous medium flows through a small and spatially varying fraction of available pores, while the bulk of it remains trapped. The trapped foam is under a pressure gradient corresponding to the pressure gradient imposed by the flowing foam and continuous wetting liquid. The imposed pressure gradient and coalescence of the stationary foam lamellae periodically open flow channels in the trapped foam region. Foam lamellae in each of these channels flow briefly, but channels are eventually plugged by smaller bubbles entering into the trapped region. The result is a cycling of flow channels that open and close throughout the trapped foam, leading to intermittent pulsing of foam flow in that region.

The dynamic behavior of foam trapped in porous media is modeled here with a pore network simulator. We predict the magnitude of the pressure drop leading to the onset of flow of foam lamellae in the region containing trapped foam. This mobilization pressure drop depends only on the number of lamellae in the flow path and on the geometry of the pores that make up this path.

The principles learned in this study allow us to predict the fraction of foam that is trapped in a porous medium under given flow conditions. We present here the first analytic expression for the trapped foam fraction as a function of the pressure gradient, and of the mean and standard deviation of the pore size distribution. This expression provides a missing piece for the continuum foam flow models based on the moments of the volume-averaged population balance of foam bubbles.

Key words: foam, mobilization, network simulation, pressure gradient, trapping, diffusion.

Nomenclature

a	pressure gradient at which half the channels are mobilized (atm/m),
A	surface area of one interface of a lamella (m^2),
b	standard deviation of calculated mobilization pressure gradients (atm/m),
B	pore shape characteristic $[1+r_t/\bar{R}_g]$,
D	diffusivity of gas through liquid phase (m^2 / s),
h	lamella thickness (m),
k	mass transfer coefficient (mol / N s),
m_y	number of clusters in the network in the flow direction,
m_z	number of clusters in the second dimension of the network,
n	moles of gas (mol),
$\dot{n}_{in}$	dimensionless moles of gas entering the network per unit time

⋆Currently at Clorox Services Company, Pleasanton, CA, U.S.A.
⋆⋆Corresponding author.

$\dot{n}_{\text{out}}$ dimensionless moles of gas leaving the network per unit time
P gas pressure (Pa),
P_{c} capillary pressure (Pa),
P_{eq} equilibrium gas pressure (Pa); pressure if all lamellae were at pore throat,
P_{u} upstream pressure (Pa),
P_{d} downstream pressure (Pa),
r_{crit} radius of curvature of a lamella at the critical position (m),
r radius of curvature (m),
r_{t} pore throat radius (m),
$\mathbf{R}$ residual vector,
R_{g} radius of cylinder used to generate an hourglass pore [grain radius] (m),
$\bar{R}_{\text{g}}$ characteristic length [average grain radius] (m),
$\mathcal{R}$ gas constant (8.314 N m / mol K),
S solubility of gas in liquid phase (mol / N m),
t time (s),
T temperature (K),
$\mathbf{u}$ solution vector made up of all lamella positions and mole values,
V bubble volume (m^3),
x dimensionless distance of a lamella from the pore throat [$-1 \leqslant x \leqslant 1$],
x_{crit} critical position,
X_{f} fraction of foam which is flowing,
X_{t} fraction of foam which is trapped,

Greek Letters

β solubility parameter [$h/\mathcal{R}TS\bar{R}_{\text{g}}$],
γ dimensionless volume [$V/\bar{R}_{\text{g}}^3$],
η dimensionless number of moles of gas [$n\mathcal{R}T/\sigma\bar{R}_{\text{g}}^2$],
Π dimensionless pressure [$P\bar{R}_{\text{g}}/\sigma$],
ρ dimensionless radius of curvature [$r/\bar{R}_{\text{g}}$],
σ liquid/gas interfacial tension (N/m),
τ dimensionless time [$tD/\bar{R}_{\text{g}}^2\beta$],
Ψ grain size distribution factor [$(\bar{R}_{\text{g}} + std)/\bar{R}_{\text{g}}$],

Subscripts

d downstream
i cluster index $\{i \epsilon (1, m_y, m_z)\}$,
j pore index $\{j \epsilon (1, 4)\}$,
u upstream

Pressure Drops

ΔP imposed pressure drop on network (Pa),
$\Delta \Pi$ dimensionless imposed pressure drop on network,
ΔP_{max} maximum pressure drop allowed across a single lamella (Pa),
ΔP_{lim} limiting mobilization pressure drop (Pa),
ΔP_{mob} dimensionless mobilization pressure drop,
ΔP imposed pressure gradient (Pa).

1. Introduction

Foam is an excellent candidate for improving oil recovery from porous media because it has a lower mobility than gas or liquid alone and therefore has a high blocking

ability. Foam in a porous medium is made up of gas bubbles that are separated by thin liquid films, called lamellae, which span across pores. When compared to continuous gas flow, foam lowers the mobility by factors as high as 5000 (Kovscek and Radke, 1994). This means that a significantly greater pressure gradient is required to keep foam lamellae flowing through a porous medium than to maintain flow of either the gas or liquid phases. In fact, experimental observations have been made of pressure gradients significantly greater than 100 psi per foot in a bead pack through which foam was flowing on the order of meters per day (Fagan, 1992).

When the imposed pressure gradient is not high enough to keep the lamellae moving, the lamellae become trapped in the pores, and gas flow is blocked. Due to the distribution of pore sizes that exists in a porous medium, foam lamellae flow in certain channels and block others where the forces to overcome trapping are not achieved (Holm, 1968; Falls *et al.*, 1989; Gillis, 1990). The trapped fraction of foam can be quite large. Tracer studies reveal that as much as 80% of the foam volume may be trapped at any time during flow (Gillis, 1990).

Hanssen and Dalland (1991) and Hansen and Haugum (1991) generated foam in a porous medium under constant pressure gradients. Foams, which they refer to as 'strong', eventually plug the porous medium and block gas flow. Gas flow reduces to a trickle, and a 'pseudo steady-state' is reached that can remain for weeks or months. Gas transport through the system is limited to diffusion through the foam lamellae. As the pressure drop across the porous medium increases, different static configurations of foam are achieved, until finally the pressure drop is high enough so that there is an onset of lamellar flow.

Our primary goal is to predict the pressure drop required to mobilize a bubble train in a porous medium. We call this the mobilization pressure drop. If it is too large, the foam is not an effective drive fluid for improved oil recovery, because there is a limit to what injection pressures can be used in the field, especially in places where well-to-well distance is very long (Rossen and Gauglitz, 1990; Friedmann *et al*., 1991).

Different predictions for the pressure drop at the onset of mobilization are presented in the literature. The highest estimate was given by Falls *et al*. (1989). They assumed that all lamellae start in pore throats; it takes a large mobilization pressure drop to move them out of the throats. Their estimates for the mobilization pressure gradient are on the order of several MPa/m. Flumerfelt and Prieditis (1988) assume an initial random distribution of lamella positions, some curved in the direction of the pressure drop and some curved against it. Therefore, they concluded that long bubble trains result in reduced mobilization pressure drops when compared to single bubbles. In fact, the mobilization pressure drop approaches zero as the inverse square root of the length of the bubble train (Prieditis, 1988).

Rossen (1990) predicted a mobilization pressure gradient between the values of Falls *et al.* and Flumerfelt and Prieditis. He correctly asserts that most lamellae are curved in the direction that resists flow, and thus there is not complete cancellation of pressure drops across oppositely curved lamellae that results in a mobilization

pressure drop of zero. Rossen defines pores as conical and derives the pressure drop that must be exceeded at the onset of mobilization. This value is greater than zero solely because of the discontinuity that occurs at the pore bodies, where there are corners. He concludes that if the pores were rounded into sinusoidal shapes, the mobilization pressure drop should approach zero. In water-wet porous media the aqueous phase congregates in corners, smoothing sharp edges. Thus, according to Rossen's argument, foams mobilize at pressures drops that are very close to zero. Only the analysis of Falls *et al.* (1989) explains why such a high fraction of foam is trapped in porous media under flow conditions with significant imposed pressure gradients.

Percolation models have employed the theories described above to predict the propagation of foams in porous media. Rossen and Gauglitz (1990) hypothesized that gas flow begins in the channel with the fewest blocking lamellae. Out of all possible pathways, the one with the minimum mobilization pressure drop must be found. The pressure drop for each pathway is the maximum pressure drop an individual lamella can withstand divided by the average distance between lamellae in the direction of flow. de Gennes (1992) considered a train of lamellae resting in the pore throats and roughly defined percolation regimes for mobilization as a function of foam density and pressure gradient. He speculated that the system remains close to the mobilization threshold because trapped regimes coarsen while bubble density increases in flowing regimes as more lamellae are formed.

Kovscek and Radke (1994) recognized the dynamic nature of foam in a porous medium. Foam which is trapped continues to evolve as adjacent bubbles coalesce. As we will illustrate, the result may be the onset of mobilization of the lamellae, allowing the foam to flow out of the pores where previously it had been trapped. In addition, foam that is free to flow may become trapped as its texture evolves. Combination of these events results in a nearly constant fraction of trapped foam during steady foam flow.

All of the theories described above which aim to predict the onset of mobilization conceptually impose a pressure gradient across a region containing trapped lamellae and increase that pressure gradient until flow begins. However, under an imposed pressure gradient, foam lamellae must continually align themselves so that the pressure drop is sustained everywhere. In other words, the Young–Laplace equation dictates which configurations of lamellae are admissible for a given imposed pressure gradient. The premise of Flumerfelt and Prieditis (1988) that lamellae are randomly distributed, is only possible when there is no pressure gradient across the bubble train. On average, however, the lamellae are in positions to resist flow, as conjectured by Rossen.

Trapped foam lamellae exert a great influence on foam mobility because they reduce the gas-phase relative permeability. In order to improve the current continuum population-balance models (Patzek, 1988; Kovscek and Radke, 1994; Kovscek *et al*., 1995), it is important to understand how foam trapping evolves with time and to predict the fraction of foam that is trapped at a set of imposed conditions.

Our earlier work (Cohen *et al.*, 1996) described a network simulation predicting much of the physics involved in the rearrangement of lamellae and changes in pressures as a result of diffusion of gas through lamellae in stationary foam. The model demonstrated that the texture of trapped foam changes with time, evolving from an initially random lamella distribution to an equilibrium configuration with a uniform final pressure. However, the issues of foam bubble mobilization and the amount of foam trapped were not addressed.

The network model presented in this paper extends our previous effort and predicts the onset of mobilization for a system of foam bubbles in a porous medium under a constant imposed pressure drop. Initially, the foam is trapped, and we predict the flux of gas that passes through the trapped lamellae as a result of diffusion. For pressure drops that remain below the mobilization pressure drop at all times, the lamellae ensemble settles to a steady state configuration. For higher pressure drops, the model predicts how long it takes for the stationary foam to mobilize and through what path the mobilization occurs. Further, we show here that as foam coarsens, the required mobilization pressure drop decreases. This effect confirms the hypothesis of Rossen and Gauglitz (1990) that the mobilization pressure drop is a function of the number of lamellae in a channel in the direction of flow. It also confirms the conclusion of de Gennes (1992) that coalescence of lamellae leads to a reduced fraction of foam which is trapped. Finally, our network model also predicts the fraction of pores in a porous medium that contains trapped foam under a given set of conditions. We present an analytic expression for the trapped fraction as a function of imposed pressure drop; this expression is a necessary component to complete the population-balance models for foam flow in porous media.

2. Foam Coarsening

A lamella residing in a water-wet pore always intersects the pore wall at a 90° angle (Bikerman, 1973; Chambers and Radke, 1990). Therefore, the lamella is always curved so that the gas pressure is higher near the throat than in the body. Gas in the bubbles on each side of a lamella is assumed to be well mixed, and thus has a uniform pressure. The pressure difference across the lamella acts as a driving force for diffusion of gas from one bubble to the next. Mass transfer through a lamella is limited by the diffusion of gas through the film, and not by the initial rate of dissolution into the film (de Vries, 1958). Hence we neglect any interfacial resistance to mass transfer. The rate of gas diffusion is described by the mass transfer equation,

$$\frac{\mathrm{d}n}{\mathrm{d}t} = -kA\Delta P; \quad k = \frac{SD}{h}, \tag{1}$$

where $\mathrm{d}n$ is the moles of gas transferred in time $\mathrm{d}t$, A is the surface area of one interface of the lamella, ΔP is the pressure drop across the lamella, defined by the Young–Laplace equation, and k is the mass transfer coefficient, which is related to the gas solubility S, its liquid phase diffusivity D, and the lamella thickness h.

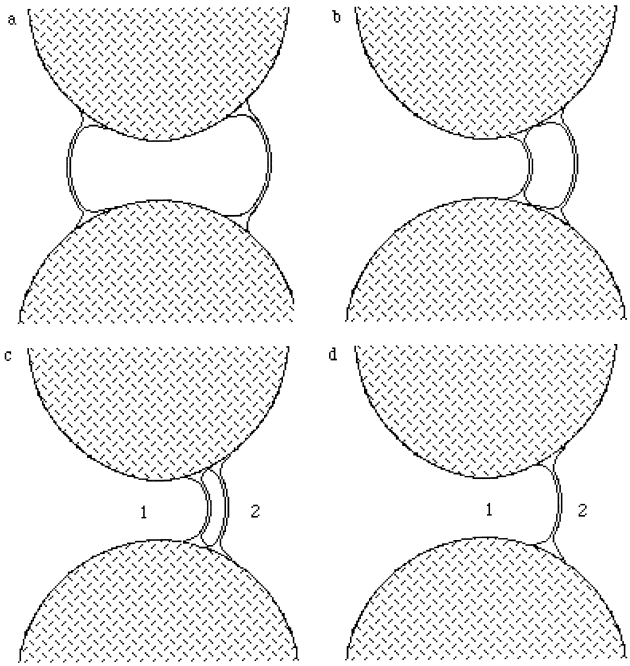

Figure 1. Schematic of the sequence of two lamellae merging into one. Cross-hatched regions corresponding to opposing solid grains. Two lamellae are moving together as a result of diffusion from the pore interior to the pore bodies. When they get close enough together, they coalesce into one lamella. The resulting single lamella is slightly farther away from the pore throat than either "parent" immediately before the merge.

As gas diffuses through a lamella, the redistribution of mass necessitates a slow translation of the lamella towards the pore throat (Cohen *et al.*, 1996). This process drives the two lamellae which were initially present in the pore toward one another until they merge and coalesce, leaving just one lamella in the pore. As the total number of lamellae decreases, so does the total number of gas bubbles between the lamellae. Hence, the bubble density of foam (texture) in the porous medium decreases. This process is known as coarsening.

Figure 1 shows the sequence of two lamellae merging together in a pore with a constant pressure drop from left to right. As gas diffuses from the bubble that spans the pore throat across the two lamellae and into the two pore bodies, the lamellae move toward one another. The lamella on the left continues to move past the pore throat so that both lamellae are on the right side of the throat just before the merge.

The minimum allowable distance between two lamellae before they coalesce is a parameter set as input to the model. Merging causes a disturbance to the system, as there must be a sudden redistribution of gas. The lamella on the higher pressure side ruptures as the two lamellae merge together. Any gas that had been between the two lamellae expands into the pore body. In Figure 1, the gas between the two

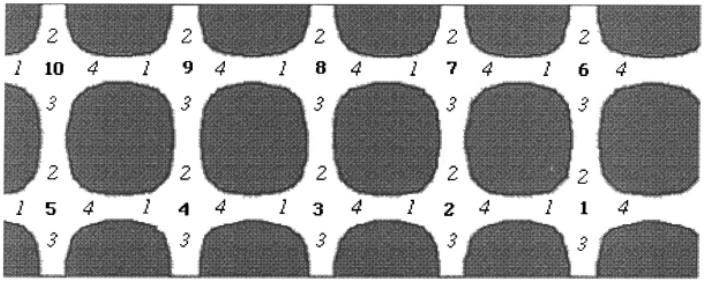

Figure 2. A 5×2 network has two channels for flow from left to right. The indexing system is illustrated here. The variables $m_y = 5$ and $m_z = 2$.

lamellae expands to the left of the remaining lamella since the leftmost lamella has ruptured. This causes the remaining lamella to jump away from the pore throat as the pressures equilibrate. In frame d of Figure 1, the resulting single lamella is to the right of the pair of lamellae in frame c. The rupture and redistribution happens very quickly and the pore body pressures on either side of the coalescence event remain nearly constant throughout. The details of the coalescence event are described in the thesis of Cohen (1996).

In a system with an initial distribution of lamellae, each pair of lamellae undergoes a merge until each pore contains only one lamella. This is the irreducible foam texture; no further coarsening occurs. Under no imposed pressure gradient, the system reaches equilibrium with all the lamellae located at the pore throats. In our current network model, however, there is an imposed pressure gradient, and the steady-state configuration is that of all lamellae residing away from the pore throats towards the downstream side of the system. In this manner, the imposed pressure gradient is sustained, and gas continues to migrate by diffusion through the trapped lamellae.

3. Model Framework

The current model is based on a two-dimensional pore network described elsewhere (Cohen *et al.*, 1996). That model predicted the behavior of randomly placed lamellae in a porous medium as they evolve to equilibrium as a result of diffusion and translation. The equilibrium configuration is one with uniform pressure everywhere. The porous medium is modeled as an array of translationally invariant hourglass-shaped pores connected together at pore bodies with a coordination number of 4. Thus, a pore is defined as the void space located between two pore bodies. The size of the array can be varied and is specified by a pair of integers describing the number of pore bodies in each dimension of the network, $m_y \times m_z$. The characteristic length, R_g, of each pore, is the radius of the grain that defines the boundary of the hourglass shape. In addition, each pore has an adjustable pore throat diameter, $2r_t$. A 5×2 network and the number scheme are illustrated in Figure 2, in which $m_y = 5$ and $m_z = 2$.

Each half-pore in the system is identified by a pair of indices (i, j), where i is the pore body number and j represents the local specific half-pore in question. An individual lamella position is defined as $x_{i,j}$, representing the fraction of the distance the lamella sits between the pore throat and the pore body. So $x_{i,j} = 0$ when the lamella is at the pore throat. If the lamella is located on the opposite side of the pore throat from pore body i, its position is negative in sign, by definition. The initial lamella configuration is reported as a vector of individual lamella positions.

The novel part of this work is the imposition of a pressure drop across the network. The pressures in the pore bodies decrease as one moves from left to right in the network. The 'upstream' and 'downstream' pressures correspond to the leftmost and rightmost pores in the network, respectively. The initial pressure conditions are specified by two input values. One is the equilibrium pressure, P_{eq}, which is the pressure achieved if the pressure gradient is allowed to relax to the equilibrium configuration, in which all the lamellae sit in pore throats and pressure is uniform everywhere (Cohen *et al.*, 1996). The second input value is the pressure gradient. This is the difference between the 'upstream' and 'downstream' pressures. In the 5×2 network illustrated in Figure 2, the pressure drop defines the identical difference in pressure between pores (5,1) and (1,4) and between pores (10,1) and (6,4).

To begin a simulation, a configuration of lamellae must be found so that the pressure drop is everywhere accomodated and the upstream pressures are the same in every row. In our modeling effort, the initial foam texture is taken as twice the equilibrium texture, which means that there are two lamellae in each pore, or one corresponding to each half-pore. An allowable initial configuration is one in which the sum of the pressure drops across all the lamellae in each row sum to the imposed system pressure drop. The technique used to find an acceptable initial configuration for a given imposed pressure drop is outlined in Appendix A.

There is a maximum pressure drop that any lamella can withstand. It is defined from the Young–Laplace equation to be

$$\Delta P_{\text{max}} = \frac{2\sigma}{r_{\text{crit}}}, \tag{2}$$

where r_{crit} is the radius of curvature of a lamella sitting at the critical position in a pore with curved walls, and σ is the interfacial tension of the gas–liquid interface. The critical position is the position at which the radius of curvature of a lamella is a minimum, and the lamella correspondingly sustains a maximum pressure drop (Cohen *et al.*, 1996). When there are two lamellae between a pair of pore bodies, neither having a negative position, the maximum allowable pressure drop between them occurs when the lamella on the lower pressure (downstream) side of the pore throat is at the critical position and the other lamella (upstream) sits at the pore throat. The maximum pressure drop across the entire network, for a system with uniform pore sizes and no lamellae having a negative position, is then

$$(\Delta P_{\text{max}})_{\text{total}} = \left(\frac{2\sigma}{r_{\text{crit}}}\right)(m_y + 1). \tag{3}$$

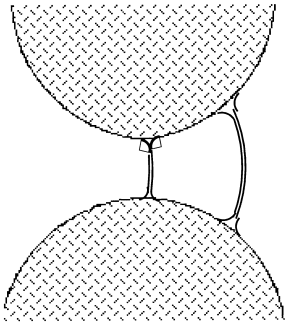

Figure 3. Pore with a pressure drop across it larger than $\Delta P_{\max}$ given by Equation (3). The lamella on the right is at the critical position and the lamella on the left is at a position such that $x < 0$.

The total pressure drop $(\Delta \mathrm{P}_{\max})_{\text{total}}$ can in fact exceed that given by Equation (3) if some pores have both lamellae on the same side of the pore throat, as illustrated in Figure 3. Thus, the actual upper bound for the maximum pressure drop between adjacent pore bodies occurs when both lamellae in the pore sit at the downstream critical position, and is double the value of $(\Delta \mathrm{P}_{\max})_{\text{total}}$ given in Equation (3). However, if this pressure difference is achieved, each pair of lamellae quickly merges together into one, and the resulting configuration no longer withstands the imposed pressure drop. Consequently, the lamellae mobilize.

Equation (3) assumes that r_{crit} is a constant. However, our network model allows for each pore to have its own unique geometry. Therefore, r_{crit} is function of the critical lamella position x_{crit} and the pore's shape parameter $B_{i,j}$, defined as

$$B_{i,j} = \left(1 + \frac{r_{\mathrm{t},i,j}}{R_{\mathrm{g},i,j}}\right) \tag{4}$$

for an hourglass pore, where $\mathrm{r}_{t,i,j}$ is the pore throat radius of the pore in question, and $\mathrm{R}_{\mathrm{g},i,j}$ is the characteristic length of that pore. Both $\mathrm{B}_{i,j}$ and x_{crit} depend on the individual pore geometry. So the more accurate expression for the maximum pressure drop across a row of hourglass pores with one lamella between each pair of pore bodies is

$$\Delta P_{\text{lim}} = \sum_{i=1}^{m_y+1} \left(\frac{2\sigma\,(x_{\text{crit}})_{i,1}}{[B_{i,1} - (1 - (x_{\text{crit}})_{i,1}^2)^{1/2}] R_{\mathrm{g},i,1}} \right). \tag{5}$$

The pressure drop defined by Equation (5) is known as the limiting mobilization pressure drop for a channel in a porous medium filled with foam. When the imposed pressure drop is below the limiting mobilization pressure drop, the lamellae remain trapped for all time.

Foam trapped in a porous medium approaches, as a result of diffusion and through coalescence events, a configuration in which there is only one lamella between each

pair of pore bodies. If the imposed pressure drop is above ΔP_{lim}, one of the coalescence events leads to the onset of mobilization. At this point, our simulator reports that flow has begun.

4. Model Definition

When a pressure gradient is imposed across a porous medium that contains foam, the foam lamellae begin to flow if the mobilization pressure drop is exceeded. Otherwise, the lamellae configure themselves in a way that resists bulk flow. It is possible that the entire medium contains only stationary foam, as in the constant-pressure-drop experiments of Hanssen and Haugum (1991). Typically, however, flow begins in some channels while the foam in other channels remains stationary. Figure 4 is a schematic diagram showing such a situation; foam flows through one channel and remains trapped in the other channels. Not shown is the aqueous wetting phase occupying the smallest flow channels.

In Figure 4, there is a pressure difference across the entire system that is determined by the behavior of the foam bubbles which are flowing. The prediction of the pressure difference has been addressed by other investigators (Kovscek and Radke, 1994). Because of the net imposed pressure difference, there is a driving force for diffusion of gas from the high pressure side of the system to the low pressure side.

The idealized porous medium that we model in this paper is shown in Figure 2. Each pore contains at least one lamella. The result of a pressure gradient imposed across the network is a diffusive flux of gas through the lamellae in the system from left to right, with gas entering through pores (5,1) and (10,1) and leaving through pores (1,4) and (6,4). The net curvature of lamellae is in the direction of the pressure gradient. This means that on average, the lamellae must be concave to the left. The pores on the far right of the network in Figure 2 extend past their pore throats so that all of the lamellae can reside on the downstream side of the pore throats at steady-state.

At the start of the network simulation, we impose a pressure drop across the system. The initial conditions, with two lamellae per pore, must be satisfied as described previously. The pressure drop across the system is held constant at all times, and is the same in all rows of the network,

$$\Delta P = P(m_y, 1) - P(1, 4) = P(2m_y, 1) - P(m_y + 1, 4). \tag{6}$$

Initially, the selected pressure drop must lie below the mobilization pressure drop for all channels in the system, so that all flow channels are blocked.

The simulator tracks the evolution of the lamellae-ensemble from its initial configuration under the influence of the imposed pressure drop ΔP. As gas diffusion occurs through the lamellae, the foam texture coarsens by lamellae merging as illustrated in Figure 1. If the imposed pressure drop is below the limiting mobilization pressure drop for all channels, the system reaches a steady-state configuration in which the remaining lamellae no longer move and gas continues to diffuse through

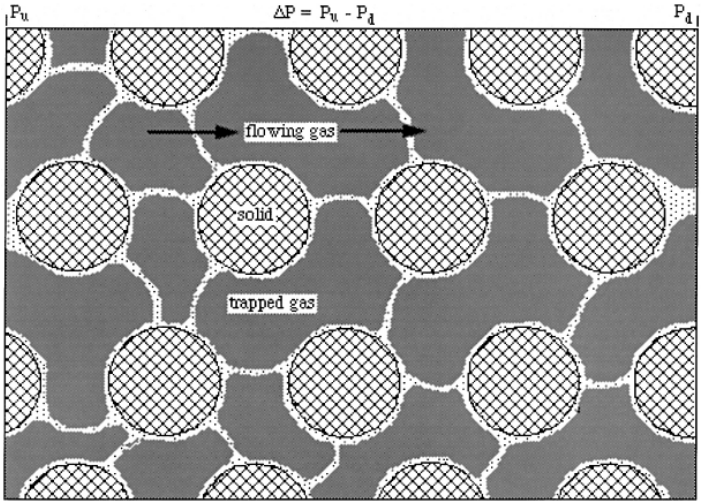

Figure 4. Schematic of foam in a porous medium under a pressure difference, ΔP, maintained between the upstream and downstream pressures (P_u and P_d). Foam bubbles flow in the largest pores but are trapped in the smaller pores since all the foam in the figure is under the influence of the same pressure gradient, and there is a resulting diffusive flux of gas through the trapped foam region. Not shown is the wetting liquid in the very smallest pore channels.

them. Otherwise, at some point, the lamellae in one of the channels mobilize before steady-state can be reached. At the onset of mobilization, our simulator stops, as it can only solve the equations for the stationary system.

The problem is solved by marching explicitly in time and solving a set of residual equations at each time step (Cohen *et al.*, 1996). The variables that must be found at each step are the lamella positions (**x**), the number of moles of gas in each bubble (**n**), the number of moles of gas entering each row on the left per unit time ($\dot{\mathbf{n}}_{\text{in}}$), and the amount of gas leaving each row on the right per unit time ($\dot{\mathbf{n}}_{\text{out}}$). Each of these quantities is a one-dimensional array of variables. The dimension of **x** is the number of lamellae in the system. The dimension of **n** is the total number of half-pores and pore bodies in the system, and the dimension of the two flow rate $\dot{\mathbf{n}}$ arrays is the number of rows m_z in the network.

For each pore body and the four half-pores that surround it, there are nine equations that must be satisfied at each time step (Cohen *et al.*, 1996). All governing equations are nondimensionalized by using the average grain radius, $\bar{R}_g$, as the characteristic length, $\sigma/\bar{R}_g$ as the characteristic pressure, and $\sigma \bar{R}_g^2/\mathcal{R}T$ as the characteristic number of moles, where $\mathcal{R}$ is the gas constant and T is temperature. Each lamella (i, j) must satisfy the Young–Laplace equation, which when substituting the ideal gas law and nondimensionalizing becomes,

$$\frac{\eta_{i,j}}{\gamma_{i,j}(x_{i,j})} - \frac{\eta_i}{\gamma_i(x_{i,k=1,4})} - \frac{2}{\rho_{i,j}(x_{i,j})} = 0. \tag{7}$$

Dimensionless volumes are indicated by γ; η represents the dimensionless number of moles; and ρ is the dimensionless radius of curvature of a lamella. Single subscripts refer to a pore body, and double subscripts refer to a particular half-pore. Each pore body has an initial volume set in the parameters of the model, but which then varies as a function of the positions of all the lamellae around it.

In addition to Equation (7), each pair of lamellae must satisfy a pair of constraints. The first constraint ensures conservation of mass in each bubble spanning a pore throat. The gas in a bubble diffuses across a lamella to a bubble at lower pressure. Since each one of these bubbles, other than those on a boundary, is surrounded by two lamellae, the equation of mass conservation is made up of the sum of two mass transfer relations, Equation (1),

$$\frac{\mathrm{d}\eta_{\mathrm{i,j}}}{\mathrm{d}\tau} + \frac{\mathrm{d}\eta_{\mathrm{k,l}}}{\mathrm{d}\tau} + 4\arccos(1 - x_{i,j}^2)^{1/2} + 4\arccos(1 - x_{k,l}^2)^{1/2} = 0, \tag{8}$$

which have been nondimensionalized after substituting expressions for A and ΔP as a function of x. Two adjacent half-pores are also related by the second constraint,

$$\frac{\eta_{i,j}}{\gamma_{i,j}(x_{i,j})} - \frac{\eta_{k,l}}{\gamma_{k,l}(x_{k,l})} = 0, \tag{9}$$

which guarantees that their pressures are equal since the gas in each bubble is well mixed. In Equations (8) and (9), half-pore (k, l) is the one that connects to half-pore (i, j).

The gas mass in each pore body in the network is also conserved,

$$\frac{\mathrm{d}\eta_{\mathrm{i}}}{\mathrm{d}\tau} - \sum_{m=1}^{4} 4\arccos(1 - x_{i,m}^2)^{1/2} = 0, \tag{10}$$

which ensures that the amount of gas transferred into or out of a pore body is equal to the amount of gas leaving or entering each of the pores around it.

Equations (7)–(10) are grouped together to constitute a vector $\mathbf{R}$ of residual equations,

$$\mathbf{R}[\mathbf{u}(t)] = \mathbf{0}, \tag{11}$$

where $\mathbf{u}$ is the solution vector made up of all the $\mathbf{x}$ and $\boldsymbol{\eta}$ values. Dimensionless time τ is defined as

$$\tau = \frac{tD}{\bar{R}_{\mathrm{g}}^2 \beta}. \tag{12}$$

The parameter β is equal to the film thickness divided by the product of the gas constant, temperature, solubility, and characteristic length. Its inverse is the conductivity of the lamella to gas transport.

In addition to the equations summarized above, there is one equation for each row in the network defining the constant pressure drop:

$$\frac{\eta_{im_y,1}}{\gamma_{im_y,1}(x_{im_y}, 1)} - \frac{\eta_{(i-1)m_y+1,4}}{\gamma_{(i-1)m_y+1,4}(x_{(i-1)m_y+1,4})} - \Delta\Pi = 0, \tag{13}$$

where i is the row number, and Π is dimensionless pressure. Also, all upstream pores must have equal pressures at all times, so

$$\frac{\eta_{im_y,1}}{\gamma_{im_y,1}(x_{im_y,1})} - \frac{\eta_{(i-1)m_y,4}}{\gamma_{(i-1)m_y,4}(x_{(i-1)m_y,4})} = 0, \quad i > 1. \tag{14}$$

There are two unknown flow rate variables per row. All but one of these are linearly independent. The constraint that defines the final flux variable ($\dot{n}_{\text{out},1}$) ensures that the total amount of gas diffusing across all the lamellae on the right equals the total amount diffusing across all the lamellae on the left,

$$\sum_i \dot{n}_{\text{in},i} = \sum_i \dot{n}_{\text{out},i}\,. \tag{15}$$

The mass transfer equations for the pores on the upstream and downstream sides of the system reflect the fact that gas enters the system on one side and exits the system on the other. In addition to gas transferred by diffusion across each lamella, gas is removed from the pores on the far right, and gas is added to the pores on the far left. For example, the equation for pore (1,4) in Figure 2 becomes

$$\frac{\mathrm{d}\eta_{\text{i},4}}{\mathrm{d}\tau} + 4\arccos(1 - x_{1,4}^2)^{1/2} + \dot{n}_{\text{out},1} = 0. \tag{16}$$

When all the equations are collected together, the unknown variables ($\mathbf{x}$, $\boldsymbol{\eta}$,$\dot{\mathbf{n}}$) are found at incremental times by marching forward using a finite difference approximation and solving at each time step using Newton–Raphson iteration. The computer code which solves the problem is listed elsewhere (Cohen, 1996).

The top and bottom boundaries of the network are handled in one of two ways. They can be thought of as dead-end pores, with no loss or addition of gas across the pore throats. In this case, the lamellae in these pores always end up at the pore throat. Otherwise, we can demand periodic boundary conditions, so that the pore throats on the bottom of the network connect to the ones on the top. Doing this does not change the fundamental result or the time scales, but it does allow for approximating the behavior of larger porous media without the computational challenge of solving for extremely large networks.

5. Mobilization Pressure Drop

Foam in a porous medium can remain stationary under an imposed pressure drop. The more lamellae there are in a potential flow channel, the higher the pressure drop that the channel can withstand. Once the imposed pressure drop is higher than the maximum allowable pressure drop, which we call the mobilization pressure drop, foam lamellae begin to flow, and our model allows us to determine the path through which flow occurs. Lamellae mobilize in the path of least resistance, which often may not be the shortest path through the porous medium, but may be a tortuous path from one end of the medium to another.

The size of the pores is also an important consideration in determining when foam mobilizes in a channel. In smaller pores, lamellae resist higher pressure drops. This can be seen from Equation (2), which shows that the maximum pressure a lamella can resist is inversely proportional to the radius of curvature of a lamella at the critical position. The radius of curvature of a lamella at a given value of x is smaller in a smaller pore, so the maximum allowable pressure is larger for these pores.

In addition to pore size, foam texture is an important consideration in determining the path of least resistance for foam. The fewer lamellae there are in a particular channel, the easier is the mobilization of the bubble train. Thus, which channel will support lamellar flow depends both on the size of the pores in the channel and the number of lamellae in the channel.

Above the mobilization pressure drop, a lamella train translates. For one lamella to flow, all lamellae around it must mobilize as well. Thus, unless the imposed pressure drop is high enough to mobilize all the lamellae in a path, the entire train of lamellae remains stationary. For a given flow path, the mobilization pressure drop, $\Delta\Pi_{\text{mob}}$, can be calculated from

$$\Delta\Pi_{\text{mob}} = \sum_{i=1}^{\ell} \left(\frac{2(x_{\text{crit}})_i \bar{R}_{\text{g}}}{[B_i - (1 - (x_{\text{crit}})_i^2)^{1/2}] R_{\text{g},i}} \right), \tag{17}$$

where $(x_{\text{crit}})_i$ and B_i are pore geometry values for the pore which corresponds to a particular lamella and the summation is over the total number of lamellae, ℓ, in the path. Equation (5) is the dimensional form of Equation (17) when there is only one lamella present per pore. Equation (17) allows any foam texture since it sums over the total number of lamellae in a flow path.

Using a single, 5-cluster long channel with uniform pore sizes, we illustrate the dependence of $\Delta\Pi_{\text{mob}}$ on the number of lamellae in a channel. Table I shows the mobilization pressure drop as a function of the number of lamellae in the channel. The mobilization pressure drops are scaled by surface tension divided by the characteristic pore size ($\sigma/\bar{R}_{\text{g}}$). Starting with 2 lamellae per pore, there are 10 lamellae initially. After all gas-diffusion driven coalescence events are complete, 6 lamellae remain. Assuming that the limiting capillary pressure for lamella rupture is not exceeded in the system (Khatib *et al.*, 1988; Jimenez and Radke, 1989), these 6 lamellae remain indefinitely in their steady-state positions. Gas continues to diffuse through the lamellae in the channel, but as long as the mobilization pressure drop is not exceeded, the 6 lamellae remain stationary.

Clearly, for a system with a uniform pore-size distribution, the mobilization pressure drop is simply the number of lamellae multiplied by the mobilization pressure drop per lamella. The dimensionless mobilization pressure drop per lamella in Table I is 3.015. The magnitude of this limiting mobilization pressure drop in pores with $R_{\text{g}} = 23\ \mu$m is about 0.045 atm per pore. So when there are 1000 pores in a row, the foam remains trapped until the applied pressure difference is 45 atm. But when R_{g}=100 μm, the limiting mobilization pressure drop is only 10 atm for 1000 pores.

Table I. Dimensionless mobilization pressure drop in a 5-cluster channel as a function of number of lamellae.

No. of lamellae	Mobilization pressure drop
10	30.15
9	27.14
8	24.12
7	21.11
6	18.09

The discrete mobilization pressure drops shown in Table I are analogous to energy levels; we call them mobilization levels. For a given number of lamellae in a channel, there is a mobilization level which, if exceeded, results in flow through the channel. For example, if the imposed pressure drop across the 5-cluster channel in Table I is $\Delta\Pi = 22$, the lamellae in the channel do not mobilize when there are 10 of them, because the mobilization level is 30.15. But as diffusion proceeds, the lamellae translate toward the throats and eventually two lamellae in a single pore approach one another and coalesce. After each merge, the mobilization level decreases. When there are 8 lamellae remaining, the mobilization level is 24.12. The imposed pressure drop of 22 is still below this level, so the trapped bubble train still does not flow. As diffusion continues, another pair of lamellae merge together. Now, the mobilization level drops to 21.11, which is below the imposed pressure drop. Immediately, the lamella train in the channel mobilizes.

This process is illustrated graphically in Figure 5, as a history of dimensionless pressure drop versus dimensionless time. The heavy dashed line delineates the imposed pressure drop, which remains constant at all times. The remaining lines show the mobilization levels as a function of time. This level is constant for a constant number of lamellae, but decreases each time a lamella merges with its neighbor. Each mobilization level is labeled with the number of lamellae that remain in the channel. When the system goes from 8 to 7 lamellae, the mobilization level drops, below the imposed pressure drop, and lamellar flow results.

Of course, the behavior of foam in a channel differs depending on the imposed pressure drop. For example, Figure 6 shows the 5-cluster, equal-pore-size channel as it behaves under an imposed pressure drop of 19 instead of 22. Not only does this change the number of lamellae which must merge before flow begins, but it changes the time scales of the events during the process. This is because the different imposed pressure drop results in a different initial configuration, so the lamellae do not merge together at the same time, and the diffusion rates are changed. Note that the lengths of the lines that represent the lifetimes of the lamellae in Figure 6 are different than the corresponding ones in Figure 5.

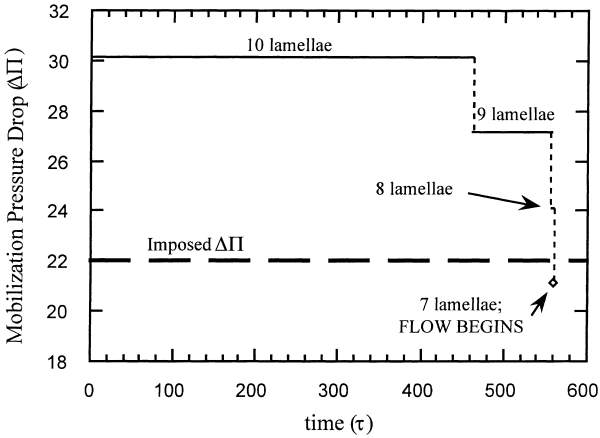

Figure 5. Mobilization levels in a 5-cluster, single channel system. After 3 of the lamellae merge with their neighbors, flow begins, because the imposed pressure drop is greater than the mobilization pressure drop for 7 lamellae in the channel.

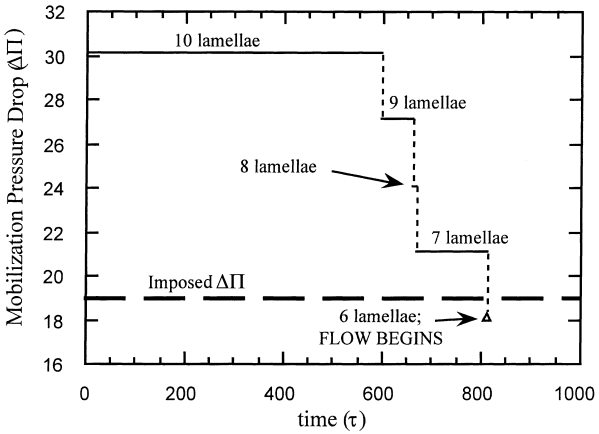

Figure 6. Mobilization levels in a 5-cluster, single channel system for lower imposed pressure drop than in Figure 5. Flow begins after 4 lamellae merge with their neighbors.

The lengths of the lines in the mobilization level history plots represent dimensionless times, which can be converted to dimensional values to discover the time scales for gas-diffusion coalescence events. For example, the first merge event in Figure 6 occurs after a dimensionless time of 600. In a porous medium with a characteristic length of 100 μm, this corresponds to 484 s. The second merge occurs less than 60 s later. Overall, the foam in the channel remains stationary for about 650 s, or just over 10 min, before the lamellae mobilize.

Clearly, the mobilization of foam in a porous medium is not as simple as some of the previous works imply (Flumerfelt and Prieditis, 1988; Falls *et al.*, 1989; Rossen and Gauglitz, 1990). If the imposed pressure drop is above the mobilization pressure

drop for the number of lamellae in a path, then flow begins immediately. Otherwise, it is possible that the onset of bubble-train flow occurs after a period of time during which diffusion-driven coarsening results in the evolution of trapped foam texture, until such time that a discrete mobilization level is exceeded. When this occurs, trapped foam flows out of a specific channel and is replaced by flowing foam from upstream. Depending on its texture, this new foam may become trapped, beginning the process again. In this way, the trapped region undergoes intermittent pulses, with foam flowing out in bursts and then trapping again as the inflowing bubble size decreases and the mobilization pressure drop is no longer exceeded.

6. Steady-State Configurations of Trapped Foam

If the imposed pressure drop is below all mobilization pressure drops, the foam lamellae never mobilize. For the 5-cluster systems of Figures 5 and 6, the pressure drop below which foam remains trapped in a channel is $\Delta\Pi = 18$. This is the limiting mobilization pressure drop as defined in Equation (5). The foam undergoes diffusion-driven coarsening until a steady-state configuration of 6 lamellae remains. At steady-state, there is a net diffusive flow of gas through the trapped foam. Figure 7 shows a system of lamellae at steady-state under a pressure drop in a network with uniform pore sizes. All of the lamellae are at the same position in their corresponding pores, and are curved to withstand the pressure drop and to allow gas to diffuse through. In a single row network, $\dot{n}_{\text{in}}$ and $\dot{n}_{\text{out}}$ are the same at steady-state.

Changing the pressure drop imposed across the channel in Figure 7 results in a different steady-state lamella configuration. As the pressure drop increases, the steady-state lamella positions approach the critical position. At $\Delta\Pi_{\text{mob}}$ for 6 lamellae, the lamellae all reside at the critical positions. Above $\Delta\Pi_{\text{mob}}$, the lamella train mobilizes.

Diffusive flow through a lamella, as defined by Equation (1), is a function of the product of the curvature of the lamella and its surface area. The surface area is a stronger function of lamella position than is curvature, and thus the diffusion flow rate continues to increase as the lamella moves away from the pore throat. The maximum diffusive flow that can pass through a lamella in this geometry occurs when the lamella is at $x = 1$, which in our model is where the pore intersects the pore body.

Table II shows how the steady-state depends on the diffusive flow rate of gas through the blocked channel in Figure 7. Increasing the molar diffusion flow rate through the channel results in steady-state lamella positions that are farther away from the pore throat. The table gives the steady-state lamella positions and the pressure drop in a 5-cluster channel as a function of diffusive gas flow. Remember that the mobilization pressure drop for this system is 18.09, so all the diffusive flow rates in Table II result in a stable stationary foam. In the table, a diffusive flow of 2.35 is the dimensionless flow rate which occurs when all the lamellae are at the critical position and the steady-state pressure drop equals the mobilization pressure drop.

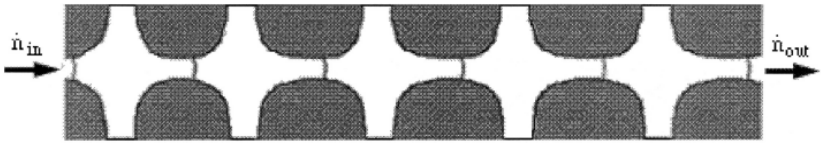

Figure 7. A 5-cluster channel under an imposed pressure gradient less than the mobilization pressure drop for 6 lamellae. At steady state, there is a diffusive flux of gas through the channel, but no hydrodynamic flow.

Table II. Steady-state lamella positions and pressure drops for increasing values of diffusive gas flux through a 5-cluster channel.

$\dot{n}$ (Dimensionless gas diffusive flow rate)	Steady-state lamella positions	Channel $\Delta\Pi$
0.5	0.125	7.20
1.0	0.247	12.85
1.5	0.366	16.31
2.0	0.479	17.84
2.35	0.554	18.09
2.5	0.585	18.05
3.0	0.635	17.83
3.5	0.768	16.48
4.0	0.841	15.31
4.5	0.902	14.08
5.0	0.949	12.87
5.5	0.981	11.71
6.0	0.997	10.60

As Table II illustrates, there are two steady-state lamella configurations possible for many imposed pressure gradients. As diffusion proceeds in an actual porous medium, the lamellae migrate toward the pore throats, and neighboring lamellae coalesce near the throats. Therefore, the more likely steady-state configurations are ones where x is smaller than the critical value. Therefore, the steady-state lamella positions are assumed to be a monotonically increasing function of pressure drop.

The fraction of the total gas flow through a porous medium due to diffusion through stationary foam depends on the magnitude of all the system variables. In a porous medium at ambient temperature with an average pressure of 1 atm, a diffusive flow rate of $\dot{n} = 1.0$ corresponds to values between 0.15 m/day for pores with $R_g = 23\ \mu$m and 0.025 ft/day for $R_g = 500\ \mu$m. The flow rates for the smaller pores seem high, but in reality, the average pressure in these systems is on the order of 10 atm or more. A factor of 10 increase in pressure lowers the dimensional flow rate by a factor of 10. So at 10 atm average pressure, the diffusive flow rate in pores with $R_g = 23\ \mu$m is 0.015 m/day. Thus, the magnitude of gas flow resulting from diffusion through stationary

pores can be significant under specific conditions, but is most often small compared to gas convection. For better comparison, Kovscek and Radke (1994) reported a Darcy velocity for gas of 0.43 m/day at an exit pressure of 47.4 atm. Using that pressure as the average pressure in the system, which is a conservative estimate, the gas flow velocity resulting from diffusion through a pore with a 5 μm throat is about 0.003 m/day.

7. Multiple Row Networks

Up until now, all the results presented have been for single channel networks. It is important to study the behavior of networks described by multiple rows, which model more realistically the behavior of foam in porous media. If all the clusters in a multiple row network are the same size, the behavior of stationary foam is the same in each row as it would be for a single channel system with the same dimensions. Therefore, the only interesting behavior in multiple row networks occurs when all the pores in the network do not have the same dimensions. In this section, we start with two-row networks where each row is made up of uniform pore sizes, but each row is different. We look at two different ratios of row sizes. After that, we investigate three-row networks with a distribution of pore sizes.

Figure 8 shows a completely blocked two-row network where each row is made up of uniform pore sizes, but the pores connecting the pore bodies in the top row are smaller than the pores in the bottom row. The pressure drop across each row is the same, and as a result the diffusive gas flow into each is different in general. The same is true for the flow out of each row. The diffusive flow through the narrower channel has to be smaller in order for it to have the same pressure drop as the wider channel. Figure 8 illustrates the behavior of the system when the imposed pressure drop is below the mobilization pressure drop for either channel. The solution vectors $\dot{\mathbf{n}}_{\text{in}}$ and $\dot{\mathbf{n}}_{\text{out}}$ are the same at steady-state in this system. The lamellae in the pores connecting the two rows merge together and situate themselves in the pore throats. Thus, the five pore bodies in the top row have the same pressures as those in the bottom row, there is no gas diffusion between the rows, and the pressure drop across each lamella in the system is the same. Since a lamella residing in a smaller pore has a smaller radius of curvature than one at the same position in a larger pore, the lamellae in the bottom row are farther from the throats than those in the top row, so all the lamellae have the same curvature. None of the lamellae exceed the critical position.

As the imposed pressure drop across the system in Figure 8 increases, lamellae eventually mobilize. Clearly, the mobilization pressure for the narrower channel is higher than that for the wider channel, so it would seem that the wider channel always mobilizes first. However, initially the lamellae in the narrower channel are closer to the pore throats in order to maintain the same pressure drop as that across the wider channel. Therefore, they may merge together sooner, causing the lamellae contained in the narrower channel to mobilize before those in the wider one. In order to determine when and where the lamellae mobilize, these two effects must be

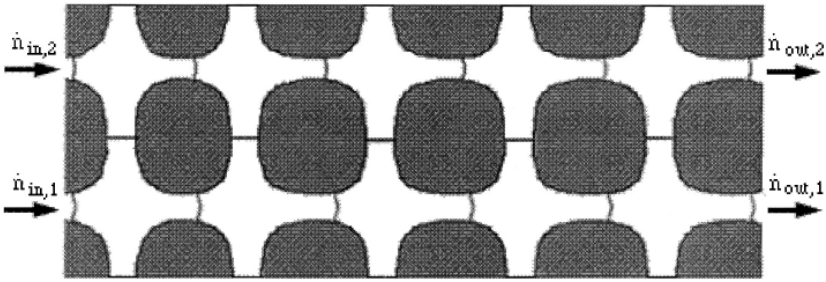

Figure 8. Steady-state configuration of a system with two 5-cluster rows under an imposed pressure gradient less than the mobilization pressure drop for either row. The top row is narrower than the bottom one, so the lamellae in the bottom row are farther away from the pore throats.

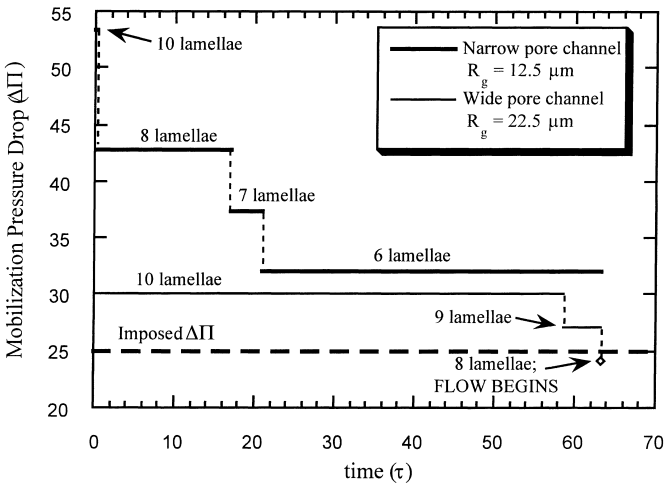

Figure 9. Mobilization levels in a 5×2 system under an imposed pressure drop of 25. The poresize in the narrow channel is 0.56 of that in the wide channel. Flow begins after 2 lamellae in the wider channel merge with their neighbors.

balanced. In which channel mobilization occurs depends on the relative pore sizes in the two channels and on the imposed pressure drop. Figure 9 gives a history of mobilization levels for the two rows of the network, similar to the analysis done in Figures 5 and 6, for a system where the pores in the narrower channel are 56% as large as those in the wider channel. The problem is scaled based on the larger pore size, and the dimensionless mobilization pressure drop is 32.06 in the narrow channel as opposed to 18.09 in the wider channel. For a pressure drop $\Delta\Pi = 25$ across the system, the wider channel mobilizes after 2 lamellae merge with their neighbors.

When the narrower channel contains pores which are 75% of the size of the pores in the wider channel and the imposed pressure drop is also $\Delta\Pi = 25$, the narrower channel mobilizes first, after the fourth merge occurs. This is because the lamellae in the wider channel are farther from the pore throats and take longer to

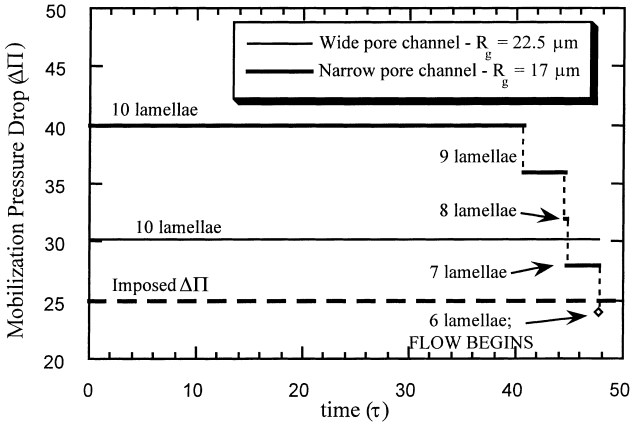

Figure 10. Mobilization levels in a 5×2 system under an imposed pressure drop of 25. The poresize in the narrow channel is 0.56 of that in the wide channel. Flow begins after 4 lamellae in the narrower channel merge with their neighbors.

merge than the ones in the narrow channel. This result is illustrated in Figure 10, in which the channels have limiting mobilization pressure drops of 23.94 and 18.09, respectively. So an applied pressure drop between 18 and 24 results in mobilization of only the wider channel, while any pressure drop above 24 results in the narrow channel mobilizing first.

The most instructive system to study is one with a distribution of pore sizes. To illustrate the effect of a pore-size distribution, a simulation has been performed on a 5×3 network with the pore sizes obeying a Gaussian distribution. The average pore size is $\bar{R}_{\mathrm{g}} = 500\ \mu$m, with a standard deviation, std $= 50\ \mu m$. In the simulation, the pore-size distribution is defined by the parameter

$$\Psi = \frac{\bar{R}_{\mathrm{g}} + \mathrm{std}}{\bar{R}_{\mathrm{g}}}, \tag{18}$$

where $\Psi = 1$ for a uniform pore size distribution. The distribution used here is $\Psi = 1.1$.

After the initial pore configuration has been defined, the system is subjected to a dimensionless pressure drop of 10, which is well below the limiting mobilization pressure drop for any row of the network. The system reaches steady state when all the lamellae merge and coalesce with their neighbors and the foam attains its minimum texture. The steady-state configuration for this 5×3 system is shown in Figure 11. Due to the non uniformity of pore sizes in each row, there now is gas diffusion between the rows. This is evidenced by the steady-state curvatures of the lamellae in the pores that are not in the lateral direction of the network.

In Figure 11, all pores are drawn to be the same size, even though they are not. The bottom row has a dimensionless limiting mobilization pressure drop of 18.25; the middle row 17.22, and the top row 20.10. In this situation, the rate of gas diffusing

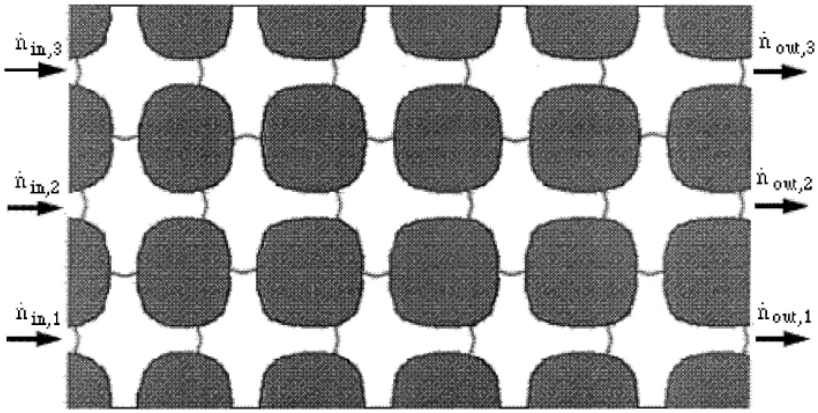

Figure 11. Steady-state configuration of a 5×3 system with Ψ=1.1 under an imposed pressure drop less than the mobilization pressure drop for any channel. There is a diffusive flux of gas between the rows.

out of each row is not the same as that diffusing into each row. In fact, the bottom row has more gas diffusing out the right than in the left, whereas the middle row has more gas diffusing in at the left than out at the right. The pressure drop across each entire row is the same, but the pressure drop across each pore is not uniform.

If the imposed pressure drop in the above 5×3 system is increased so that it is above at least one of the limiting mobilization pressure drops, we can learn much about the mobilization of real systems. For example, we can find out whether or not mobilization always occurs in straight channels, through a minimal number of pores, or perhaps through more tortuous paths. Figure 12 shows a plot of mobilization levels during the merge and coalescence process for the network of Figure 11 under an imposed pressure drop of 20. This type of analysis only takes into consideration the mobilization pressures through horizontal channels of the network. If the mobilization level for any of these channels falls below the imposed pressure drop, the lamellae in the horizontal row mobilize. Vertical spacing between mobilization levels is not uniform anymore because each pore is of a different size and thus adds a unique contribution to the mobilization pressure drop.

In the case illustrated by Figure 12, the bubble train mobilizes after the merge of lamella (10,4) with its neighbor at $\tau = 1530$. But the mobilization level of the second straight channel is still above the imposed pressure drop. The plot of mobilization levels does not take into account more tortuous flow paths. In this case, mobilization does not simply occur in the second row of the network, but through another path that contains pore (10,4). In order to determine the specific mobilization path, it is necessary to calculate the mobilization levels for all possible paths containing pore (10,4). This is done by adding the mobilization pressure drops of all lamellae that are in the flow direction. There is no contribution from lamellae in the vertical pores. If one of the paths has a level below the imposed pressure drop, then it is the one

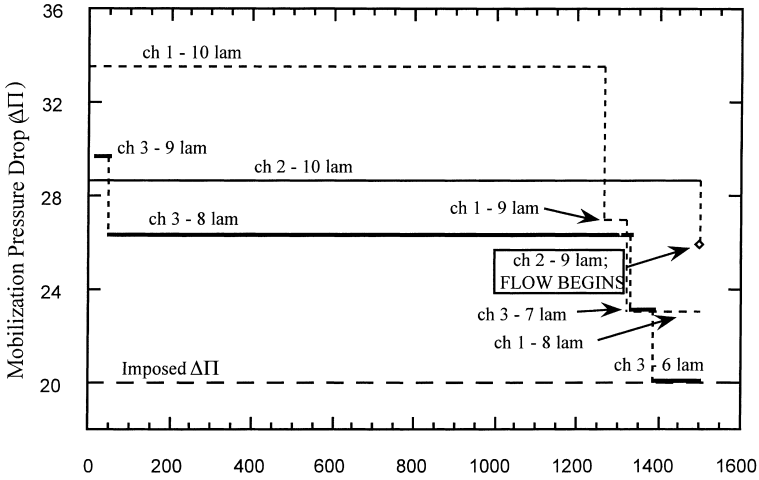

Figure 12. Mobilization levels in a 5×3 system with $\Psi = 1.1$. In this case, mobilization occurs when the mobilization levels in all three straight channels are higher than the imposed pressure drop.

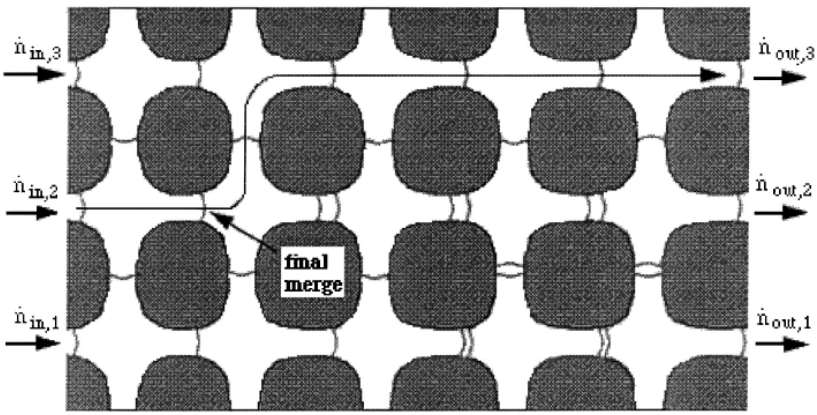

Figure 13. Lamella configuration at the point of mobilization in a 5×3 network with $\Psi = 1.1$. Upon the coalescence of two lamellae at the labeled position, the path marked with a long arrow mobilizes through the system.

through which lamellae mobilize. In this particular example, the path is found by summing the contributions of pores (10,1), (9,1), (13,1), (12,1), (11,1), and (11,4). At the onset of mobilization, the mobilization level of this path is 19.09, which is below the imposed pressure drop of 20. The channel also includes pore (9,2), but this pore is perpendicular to the flow direction, so it is not included when summing the contributions to the mobilization level. Figure 13 shows the lamella configuration at the time of mobilization. The figure only indicates the presence of two or one lamellae in a pore; it does not reflect the exact positions of the lamellae. The long arrow shows the channel through which lamellae flow at the onset of mobilization.

The location of the final merge and coalescence event that triggered hydrodynamic flow is also marked.

8. Foam Trapping

The physical understanding gained here into the mobilization of foam in porous media is useful in augmenting the effort to model foam flow. In their continuum models, Patzek (1988), Friedmann *et al.* (1991), Kovscek and Radke (1994), and Kovscek *et al.* (1995) did not describe accurately the physical characteristics of the region of trapped foam under varying conditions. As we have previously discussed, if the pressure drop across a region of a porous medium is below the limiting mobilization pressure drop, the foam in that region remains stationary. The network simulator used here investigates the transient behavior of foam of a given texture in a finite size region of pores of a particular geometry and under a fixed pressure drop. If the limiting mobilization pressure drop is exceeded, foam lamellae eventually mobilize. When mobilization occurs, the simulation run is complete, and it is possible to determine which path the flowing foam follows.

Under a given pressure drop, foam of a given texture flows through a certain fraction of pores. Other channels contain foam that is trapped and intermittently flows as its texture coarsens to below the critical texture, corresponding to the limiting mobilization pressure drop. Finally, there is a fraction of the pores which contain foam that is trapped at all times. Given the information presented earlier, it is possible to calculate this fraction as a function of applied pressure gradient and for various pore-size distributions and capillary entry pressures.

Since the mobilization pressure drop is calculated by adding the pressure drops sustained by each lamella were it located at the critical position, there is a critical number of lamellae, corresponding to a critical foam texture, below which foam mobilizes through a channel. For any single channel, the critical texture depends on the geometry of each of the pores between the two ends. If the initial texture is above the critical texture, but the equilibrium texture, where all lamellae sit at the pore throats, is below the critical texture, foam mobilizes through the channel after a period of diffusion-driven coarsening.

If the equilibrium texture is above the critical texture for the given pressure drop, foam remains trapped in the channel at all times. Our goal is to predict the fraction of foam that remains trapped at any given pressure drop. To do this, a porous medium is defined as a collection of flow channels connecting one end of the medium with the other. Each channel is made up of a linear combination of pores of various sizes and has about the same total length. Each channel then has a corresponding pressure drop which is required to move foam of a given texture through it. Some channels, those with more large pores, mobilize at relatively low pressure drops, while others require higher pressure drops. By sampling a sufficiently large number of these channels, a representative fraction of channels that are mobilized at any given pressure gradient can be calculated.

The maximum steady-state foam texture has one lamella in each pore. Any denser texture eventually coarsens to this one as a result of diffusion and merging. In our subsequent calculations we use the maximum steady-state foam texture. Actual porous media may contain foam with fewer than one lamella in each pore. In that case the mobilization pressure is lower, and thus the fraction of foam which flows is higher.

The result of this calculation depends on the pore-size distribution selected. It is generally accepted that a skewed distribution, such as the lognormal distribution (Aitchison and Brown 1957) or the Weibull distribution (Mohanty and Salter 1982) well describes pore-size distributions in a porous medium. For simplicity, we choose the lognormal distribution here, with a mean characteristic pore size, $\bar{R}_g$, and a given standard deviation. Randomly generated pores are placed in a row until the predetermined length is exceeded. Each pore and surrounding pore body is assumed to have a length of $4\bar{R}_g$. The predetermined length of the channel is the length taken up by 20 pores with the average characteristic length. Therefore, the minimum channel length is $80\bar{R}_g$. Some channels are made up of fewer than 20 pores, and some have slightly more than 20 pores.

Each channel has a capillary entry pressure. This is the pressure that must be exceeded for gas to displace completely liquid which initially occupies a channel. Only above the capillary entry pressure can foam lamellae be formed in a channel. Liquid drainage out of a pore is controlled by the pore throats (Wardlaw *et al.* 1987). Therefore, in order for foam to occupy a channel, the capillary pressure must overcome that required to displace water from the smallest pore in the channel or

$$P_c = \frac{2\sigma}{r_{t,\min}}, \tag{19}$$

where $r_{t,\min}$ is the radius of the smallest pore throat. In our geometry, the pore throats are one-fifth of the characteristic pore size, $r_t = 0.2\bar{R}_g$.

The calculations that follow are for a lognormal distribution with $\bar{R}_g$ = 100 μm and a standard deviation of 50 μm. The complete pore-size distribution is shown in Figure 14. We proceed by creating 1000 channels, just over 8 mm in length, consisting of a random sample of the pores. For all the pores to be occupied by foam, a capillary entry pressure of 0.182 atm must be exceeded at a surface tension of 35 mN/m. The limiting mobilization pressure drop of each channel is calculated and divided by the length of the channel, in order to represent a pressure gradient. The computer program used to establish these mobilization pressure gradients is reproduced in the thesis of Cohen (1996).

The percentage of pores that contain flowing lamellae is calculated as a function of imposed pressure gradient, as shown in Figure 15 by a normal probability plot. The y-axis of this plot represents a normal distribution around the mean value of 50%. The shape of the graph indicates that at low pressure gradients, an increase in pressure generates a small increase in the number of channels mobilized. The same is true at high imposed pressure gradients. Most of the foam makes the transition

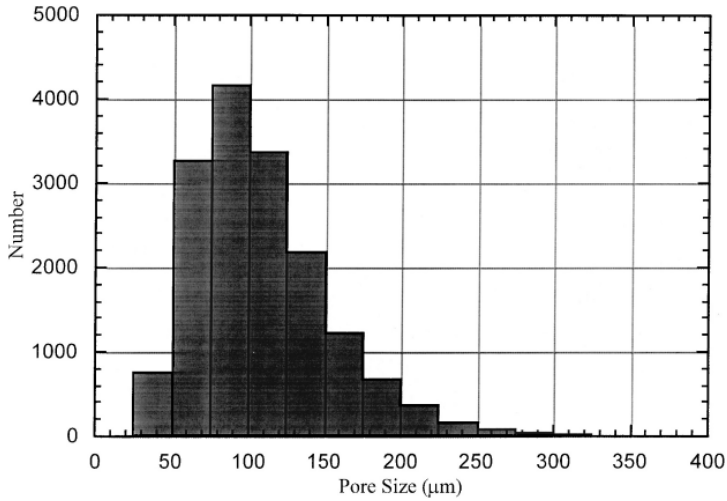

Figure 14. Lognormal pore size distribution used for trapped fraction calculated. The mean characteristic pore size is 100 μm.

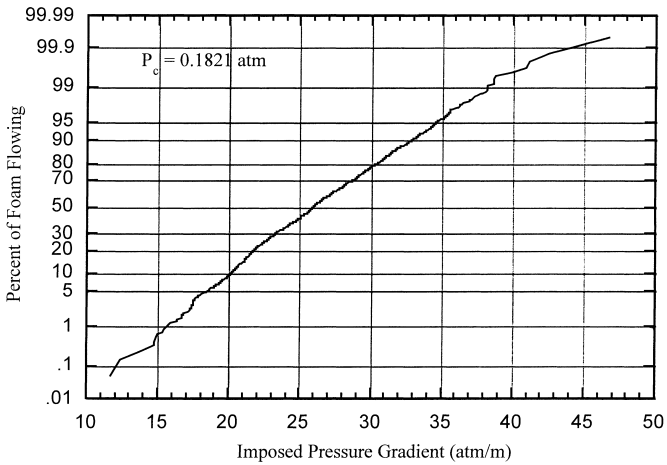

Figure 15. Percentage of flowing foam as a function of mobilization pressure gradient with a capillary entry pressure of 0.182 atm in a porous medium made up of pores distributed as in Figure 14.

from trapped to flowing at intermediate imposed pressure gradients. Half of the foam is mobilized at an imposed pressure gradient of 26 atm/m.

The data in Figure 15 are for a system which is at a capillary entry pressure such that all the pores are invaded by foam. If the capillary entry pressure is below this value, only those pores with pore throats above a corresponding value can be invaded by gas. Therefore, to find out how the mobilization curve varies as a function of capillary entry pressure, only channels which contain pores that are large enough

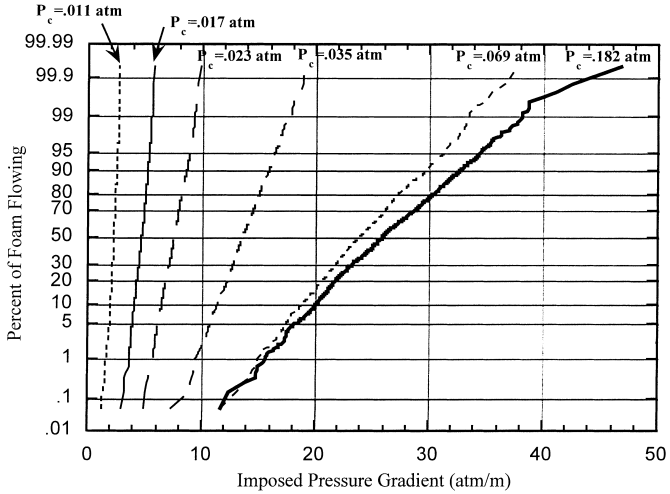

Figure 16. Percentage of foam in porous media that is mobilized as a function of mobilization pressure gradient for various capillary entry pressures. A fraction of the total number of pores is occupied by foam at a given capillary pressure. All of the pores are occupied by foam at P_c=0.182 atm.

to be invaded at the particular capillary pressure can be used. As pores are randomly selected to be placed in channels, a pore is only selected by the program if it can be invaded under the capillary pressure conditions. The same pore-size distribution (c.f., Figure 14) is adopted but only pores above a given cutoff are used to construct the channels. Figure 16 shows the same data as Figure 15, but for 5 different values of capillary entry pressure. These values correspond to using a surface tension of 35 dyne/cm and pores larger than 250, 200, 150, 100, 50, and 0 μm, respectively, ordered from left to right on the plot. The 0 μm case is the situation when all pore sizes are allowed, the same as in Figure 15.

It is clear that for lower capillary entry pressures, the mobilization pressure gradient needed to overcome trapping is reduced. From Figure 16, we see that for a capillary entry pressure of 0.011 atm, all the channels that contain foam are mobilized under a pressure gradient of 2.5 atm/m, as compared to about 50 atm/m needed to mobilize all the channels at the highest capillary entry pressure. In order to mobilize foam in a porous medium when a limited pressure driving force is available, either a small fraction of the total porous medium must be invaded by gas, i.e., the capillary entry pressure is low, or the foam texture must be very coarse, i.e., only one lamella exists for every 10 or more pores in the system. The results in Figure 16 are for the highest equilibrium foam texture, which is one lamella per pore.

It is possible to derive an analytical expression for mobilization curves such as the ones in Figures 15 and 16. These curves can also be presented as a distribution of mobilization pressure drops for all the channels sampled in the study. The mean pressure gradient, a, is the imposed pressure drop at which half of the channels in the

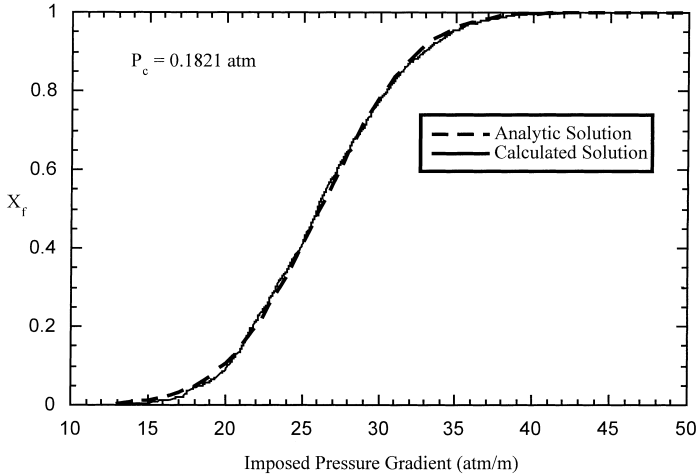

Figure 17. Flowing foam fraction as a function of mobilization pressure gradient with a capillary entry pressure of 0.182 atm, plotted using a linear scale. Also included is the curve described by the analytical expression; $a = 26.141$ atm/m and $b = 4.94$ atm/m.

system are mobilized. The standard deviation of the pressure gradient distribution is b. The flowing fraction, X_f, is a function of mobilization pressure gradient,

$$X_f = \tfrac{1}{2}\mathrm{erfc}\left(\frac{a-|\nabla P|}{b\sqrt{2}}\right). \tag{20}$$

Given the pore geometry, the pore-size distribution, and the capillary entry pressure, a simple program finds the mean and standard deviation of mobilization pressure gradients, a and b, respectively, which then can be used to find the fraction of foam that is trapped, X_t $(= 1 - X_f)$, under a given pressure gradient. This result can in turn be used in existing continuum population balance models (Patzek, 1988; Kovscek and Radke, 1994; Kovscek *et al.*, 1995).

Figure 17 shows the same information as Figure 15, but plotted on a linear scale. Shown are the data and the fit using Equation (20). The data for the 0.182 atm capillary pressure case have a mean mobilization pressure gradient of 26 atm/m and a standard deviation of 4.9 atm/m.

9. Summary

A simple two-dimensional network model of hourglass pores, first developed elsewhere (Cohen *et al.*, 1996), has been adapted here to show how stationary foam in a porous medium adjusts under the influence of a constant pressure gradient. The lamellae arrange themselves so as to resist the imposed pressure drop, allowing only a net diffusive flow of gas from the high pressure side of the network to the low pressure side. We model the evolution of the lamellae ensemble, leading to either a steady-state configuration or eventually to the onset of mobilization of some of the lamellae in the system. Our results can be summarized as follows:

- There is a maximum pressure drop that a train of lamellae can withstand in a series of pores, called the mobilization pressure drop. This maximum pressure drop is a function of the number of lamellae in a channel and is calculated by noting that each lamella can withstand a pressure drop limited by its critical position. When all possible flow paths are subject to applied pressure drops below the mobilization pressure drops the foam remains trapped throughout the entire region.
- Our model assumes a minimum lamella density of one lamella per pore. The initial lamella density is twice this value, but diffusion leads to coarsening, leaving one lamella in each pore. The mobilization pressure drop corresponding to the minimum lamella density is called the limiting mobilization pressure drop. When this value is exceeded, lamellae begin to flow. Otherwise, mobilization cannot occur.
- The steady-state configuration in this case is one which has a constant diffusive flux of gas through the stationary lamellae, which remain at positions away from the pore throats. This steady-state behavior was observed experimentally in the constant-pressure foam flow experiments of Hanssen and Haugum (1991).
- Above the limiting mobilization pressure drop, foam eventually mobilizes through a particular path in the porous medium after a series of merge and coalescence events. As each lamella merges with its neighbor, the mobilization level for each path which contained the lamella decreases, and if one of these levels falls below the imposed pressure drop, flow begins. This process is illustrated by mobilization level history plots.
- When the mobilization level is exceeded and mobilization begins through a particular channel, foam bubbles flow out of that channel and are replaced by a finer-textured foam from upstream. This foam then traps in the open channel and the diffusion-driven coarsening process begins again until another channel, or possibly the same one, has its mobilization level decrease below the imposed pressure drop. For systems with average pore sizes of about 100 μm, this entire cycle occurs in about 10 min.
- Based on the predictions of our model, it is possible to predict the fraction of foam that is trapped in a porous medium under a given pressure gradient, and given a representation of the pore-size distribution. We present an analytic expression for the fraction of foam which is trapped at any imposed pressure gradient. Such information is necessary for predictive modeling of foam flow in porous media.

Appendix A. Initial Conditions

The first challenge in solving the constant pressure-drop problem is to find an initial lamella configuration that satisfies the initial condition parameters. Imposing a specific pressure drop on the network severely restricts the possible lamella positions.

A robust algorithm has been developed (Cohen, 1996) to find an acceptable initial configuration, given the imposed pressure drop on the network.

Given the upstream and downstream pressures and the lamella positions in the upstream and downstream pores, the pore body pressures on the upstream and downstream sides of network are found. Then the initial condition generator sweeps the network one pore body at a time and finds acceptable lamella positions assuming that there are two lamellae between each pair of bodies.

The first row of the network has a uniform decrease in pressure from one pore body to the next. After calculating the pressures in the upstream and downstream pore bodies, the remaining pressure drop is divided into equal portions to find the uniform decrease. The fact that the pore-body pressures are set puts constraints on the positions of the two lamellae in the pore connecting the adjacent bodies. Given the pore-body pressures and the position of one of the lamellae between them, the position of the other lamella is fixed. The radius of curvature of this lamella is calculated from the Young–Laplace equation and the corresponding lamella position is calculated from

$$x_{i,j} = \frac{B_{i,j}\rho_{i,j}R_{\mathrm{g},i,j}\bar{R}_{\mathrm{g}} \pm \sqrt{R_{\mathrm{g},i,j}^4 - B_{i,j}^2 R_{\mathrm{g},i,j}^4 + \rho_{i,j}^2 R_{\mathrm{g},i,j}^2 \bar{R}_{\mathrm{g}}^2}}{(\rho_{i,j}^2 \bar{R}_{\mathrm{g}}^2 + R_{\mathrm{g},i,j}^2)}, \tag{A.1}$$

where $B_{i,j}$ is the pore shape parameter, $\rho_{i,j}$ is the dimensionless radius of curvature of the lamella, $R_{\mathrm{g},i,j}$ is the characteristic length of the pore in question, and $\bar{R}_{\mathrm{g}}$ is the average characteristic pore length for the network. It is possible that there is no solution to Equation (A.1) for a given set of conditions. In this case, the other lamella must be moved around until a solution is found.

Subsequent rows in the network are set so that the upstream and downstream pressures are the same in every row. In each row, other than the first, the pore bodies do not have uniform pressure differences between them. The initial configuration in each row is calculated one pore body at a time. For each pore body, there are four lamellae that must be positioned, two between the current pore body and the one in the row below and two between the current pore body and the upstream pore body. These lamellae are placed so as to give an appropriate value of the pore body pressure. The only constraint for this pressure is that the remaining lamellae must be able to withstand enough of a pressure difference so that the last downstream pore body has the proper pressure.

Once a satisfactory configuration of lamellae has been achieved to handle the desired pressure drop, the pressures and mole contents of each bubble are calculated. First, the pressure in one bubble is arbitrarily set and all the other pressures are calculated from the Young–Laplace equation. For these pressures, the number of moles in each bubble is calculated, given the volume of each bubble. The moles and pressures

are then adjusted in order to satisfy the prescribed equilibrium pressure. This is done by calculating from the equilibrium pressure, P_{eq}, the number of moles, N,

$$N = \frac{P_{\mathrm{eq}} V_{\mathrm{t}}}{\mathcal{R}T}, \tag{A.2}$$

where V_{t} is the total volume of the system. The number of moles of gas in bubble i is adjusted by the equation

$$n_{i,\mathrm{new}} = n_{i,\mathrm{old}} + cV_i, \tag{A.3}$$

where V_i is the volume of the bubble i and $N = \sum_j n_{j,\mathrm{new}}$. The constant c is

$$c = \frac{N - \sum_k n_{k,\mathrm{old}}}{V_t}. \tag{A.4}$$

The initial configuration so obtained is one of the allowable configurations for the network under the imposed pressure gradient. The initial conditions are much less random than they were for the systems studied in the previous work (Cohen *et al.*, 1996). The lamella configuration portrays a net curvature that is convex toward the downstream side of the network. In other words, lamellae arrange themselves to sustain an imposed pressure drop. The convex configuration resists flow under the imposed pressure drop until the foam in the channels coalesces and fewer lamellae remain to resist flow.

Acknowledgements

This work was funded by the Assistant Secretary for Fossil Energy, Office of Oil, Gas, and Shale Technologies of the U.S. Department of Energy under Contract No. DE-AC03-76SF00098 the Lawrence Berkeley National Laboratory.

References

Aitchison, J. and Brown, J. A. C.: 1957 *The Lognormal Distribution*, Cambridge University Press, Cambridge.

Bikerman, J. J.: 1973, *Foams*, Springer-Verlag, Berlin.

Chambers, K. T. and Radke, C. J.: 1990, Capillary phenomena in foam flow through porous media, In: N. R. Morrow (ed.), *Interfacial Phenomena in Petroleum Recovery*, Marcel Dekker, New York, Chap. 6, pp. 191–255.

Cohen, D., Patzek, T. W. and Radke, C. J.: 1996, Two-dimensional network simulation of diffusion driven coarsening of foam inside a porous medium, *J. Coll. Interf. Sci.* **179**, 357–373.

Cohen, D.: 1966, PhD Thesis, University of California at Berkeley.

de Gennes, P. G.: 1992, Conjectures on foam mobilization, *Revue de L'Institut Francais du Petroll* **47**(2), 249–254.

de Vries, A. J.: 1958, Foam stability: Part II, gas diffusion in foams, *Recueil* **77**, 209–461.

Fagan, M.: 1992, MS Thesis, University of California at Berkeley.

Falls, A. H., Musters, J. M. and Ratulowski, J.: 1989, The apparent viscosity of foams in homogeneous bead packs, *SPE Res. Eng.* **4**(2), 155–164.

Flumerfelt, R. W. and Prieditis,: 1988, Mobility of foam in porous media, In: D. H. Smith (ed.), *Surfactant-Based Mobility Control*; ACS Symposium Series 373, American Chemical Society, Washington, DC, Chap. 15, pp. 295–325.

Friedmann, F., Smith, M. E. and Guice, W. R.: 1991, Steam-form mechanistic field trial in the Midway-Sunset Field, SPE 21780, Presented at the Western Regional Meeting of the SPE, Long Beach, CA, March 1991.

Gillis, J. V.: 1990, PhD Thesis, University of California at Berkeley.

Hanssen, J. E. and Dalland, M.: 1991, Foam barriers for thin oil rims: Gas blockage at reservoir conditions, Presented at *6th European Symp. on Improved Oil Recovery*, Stavanger, 21–23 May, 1991.

Hanssen, J. E. and Haugum, P.: 1991, Gas blockage by non-aqueous foams, SPE 21002, Presented at *SPE Int. Symp on Oil-Field Chemistry*, Anaheim, CA.

Holm, L. W.: 1968, Mechanism of gas and liquid flow through porous media in the presence of foam, *Soc. Petr. Eng. J.* **8**(6), 359.

Jimenez, A. I. and Radke, C. J.: 1989, Dynamic stability of foam lamellae flowing through a periodically constricted pore, In: J. K. Borchardt and T. F. Yen (eds), *Oil-Field Chemistry; Enhanced Recovery and Production Stimulation*; ACS Symposium Series 396, American Chemical Society, Washington DC, Chap. 25, pp. 461–479.

Khatib, Z. I., Hirasaki, G. J. and Falls, A. H.: 1988, Effects of capillary pressure on coalescence and phase mobilities in foams flowing through porous media, *SPE Res. Eng.* **3**, 919–926.

Kovscek, A. R. and Radke, C. J.: 1995, Fundamentals of foam transport in porous media. In: Laurier L. Schramm (ed.), *Foams: Fundamentals and Applications in the Petroleum Industry*; Advances in Chemistry Series 242, Chap. 3, pp. 113–163.

Kovscek, A. R., Patzek, T. W. and Radke, C. J.: 1994, Mechanistic prediction of foam displacement in multidimensions: A population balance approach, *Chem. Eng. Sci.* **50**(23), 3783–3799.

Mohanty, K. K. and Salter, S. J.: 1982, Multiphase flow in porous media: Pore-level modeling, SPE 11017, 11018, Presented at *57th Annual Fall Technical Conf. and Exhibition of the SPE of AIME*.

Patzek, T. W.: 1988, Modeling of foam flow in porous media by the population balance method, In: D. H. Smith (ed.), *Surfactant-Based Mobility Control*, ACS Symposium Series 373, American Chemical Society, Washington DC, Chap. 16, pp. 326–341.

Prieditis, J.: 1988, PhD Thesis, University of Houston.

Rossen, W. R.: 1990, Theory of mobilization pressure gradient of flowing foams in porous media (Parts i, ii, iii), *J. Coll. Interface Sci.* **136**(1), 1–53.

Rossen, W. R. and Gauglitz, P. A.: 1990, Percolation theory of creation and mobilization of foams in porous, *AIChE J.* **36**(8), 1176–1188.

Wardlaw, N. C., Li, Y. and Forbes, D.: 1987, Pore-throat size correlation from capillary pressure curves, *Transport Porous Media* **2**, 597–614.